[7] S. S. Attwood, "Surface-wave propagation over a coated plane conductor," *J. Appl. Phys.*, vol. 22, no. 4, pp. 504–509, 1951.
[8] K. N. Rozanov, "Ultimate thickness to bandwidth ratio of radar absorbers," *IEEE Trans. Antennas Propag.*, vol. 48, no. 8, pp. 1230–1234, 2000.
[9] B. A. Munk, *Frequency Selective Surfaces*. New York, NY, USA: Wiley, 2005.
[10] C. L. Holloway *et al.*, "Use of generalized sheet transition conditions to model guided waves on metasurfaces/metafilms," *IEEE Trans. Antennas Propag.*, vol. 60, no. 11, pp. 5173–5186, 2012.
[11] R. E. Collin, *Foundations for Microwave Engineering*. New York, NY, USA: Wiley, 2001.
[12] G. Goussetis *et al.*, "Artificial impedance surfaces for reduced dispersion in antenna feeding systems," *IEEE Trans. Antennas Propag.*, vol. 58, no. 11, pp. 3629–3636, 2010.
[13] W. B. Weir, "Automatic measurement of complex dielectric constant and permeability at microwave frequencies," *Proc. IEEE*, vol. 62, no. 1, pp. 33–36, 1974.

A Dual Circularly Polarized Waveguide Antenna With Bidirectional Radiations of the Same Sense

Yang Zhao, Zhijun Zhang, Kunpeng Wei, and Zhenghe Feng

***Abstract*—A dual circularly polarized waveguide antenna with bidirectional radiations of the same sense is proposed in this communication. Bidirectional circular polarization (Bi-CP) of the same sense was obtained by two identical rectangular metal slices installed on one lateral side of the waveguide with an intersection angle of 45°. These two metal slices were horizontally perpendicular to each other and vertically spaced by a quarter guided wavelength. A rat-race coupler was employed to excite the two metal slices with the same amplitude, but with a 0° or 180° phase difference depending on the selection of two inputs. One sense of Bi-CP was realized when the two metal slices were fed in phase and the opposite sense of Bi-CP could be obtained when they were fed out of phase. A prototype for 2.4-GHz WLAN application was tested to verify our design. The measured common bandwidth for 10-dB return loss and 3-dB axial ratio at the two feed ports was 230 MHz (9.6%, 2.29–2.52 GHz) and 210 MHz (8.6%, 2.35–2.56 GHz), respectively. The measured isolation between the two feed ports was better than 30 dB over the whole operating band.**

***Index Terms*—Bidirectional, circular polarization, dual sense, same sense.**

I. Introduction

Circularly polarized antennas are usually required in many wireless communication systems because they can allow the avoidance of polarization alignment between the transmitting (Tx) and receiving (Rx) terminals and thus enhance link consistency, which is advantageous in comparison to linearly polarized ones. In principle, circularly polarized waves are usually excited by two orthogonal linearly polarized components with the same amplitude, but with a 90° phase difference. The practical designs of antenna with circular polarization (CP) include single-fed method with structural perturbation, dual-fed technique, and structural rotation of several linearly polarized elements [1]–[3], etc. Meanwhile, a single antenna operating with both senses of CP [4]–[8] is much preferred for the reason that it can integrate the traditionally separated Tx and Rx antennas into one and thus reduce system complexity. Besides, the adoption of two orthogonal signals with dual senses of CP, in this case left-hand CP (LHCP) and right-hand CP (RHCP), also allows a more efficient utilization of the electromagnetic spectrum and increases the link capacity. A patch antenna coupled by two crossed slots with four arms serially fed by a single microstrip line was proposed in [4] to realize dual senses of CP through the excitation at either end of the microstrip line. A planar dual circularly polarized array was presented in [5] whose element comprises an arc-shaped patch and an extended stub, and it can radiate LHCP or RHCP depending on the feed port that was selected. An open-end waveguide integrated with a septum polarizer was proposed in [6]–[8] to achieve dual CP senses, and two individual coaxial ports were located at the two sides of the septum for both senses of CP. But all these designs focus on unidirectional radiation with both senses of CP.

On the other hand, bidirectional CP (Bi-CP) is needed in various modern wireless applications, such as a microcellular base station, a radio frequency identification system, an indoor high-speed WLAN, a coal mine channel, a bridge or tunnel communication, etc. Slot radiators are good candidates for Bi-CP and have been studied by many researchers. However, the existing design will produce CP of opposite senses in the two different radiating directions [9]–[11]. This means that if an LHCP is produced at one end, RHCP would unavoidably be generated at the opposite end. No information can be exchanged if the polarizations are mismatched in that opposite direction. For the realization of CP of the same sense in the two opposite directions, a back-to-back arrangement by two circularly polarized patch elements was proposed in [12]–[14]. In [12], a slot-coupling feeding approach was utilized to excite two back-to-back corner-cutting circularly polarized patches. A coplanar waveguide feeding structure was employed in [13], [14] to excite two back-to-back partially overlapped rectangular patches for Bi-CP of the same sense. However, these designs are realized just by replicating and superposing unidirectional circularly polarized elements located at the front and back sides of a common feeding scheme, and they have insufficient axial ratio bandwidth. A waveguide antenna with Bi-CP of the same sense was designed in [15], but only one sense of CP was available. In addition, the realization of dual senses of CP with bidirectional radiations of the same sense has not been published in literature.

In this communication, we propose a novel design of dual circularly polarized waveguide antenna with bidirectional radiations of the same sense for either CP. Both senses of CP are obtained for a single antenna by selecting two different input ports. The proposed structure incorporated two rectangular metal slices installed inside a square-aperture waveguide, as that proposed in [15]. These two metal slices were perpendicular to each other in the horizontal plane, and separated by a quarter guided wavelength in the vertical direction. For the realization of dual senses of CP, a rat-race coupler was used in this study to feed the two metal slices along their diagonal line with the same amplitude, but with a 0° or 180° phase difference. When the two metal slices were fed with the same phase, one sense of Bi-CP was realized, but Bi-CP of the opposite sense could be obtained when they were fed with anti-phase. The design details are presented in the following sections.

Manuscript received April 13, 2013; revised September 17, 2013; accepted October 14, 2013. Date of current version December 31, 2013. This work was supported in part by the National Basic Research Program of China 2010CB327400, in part by the National High Technology Research and Development Program of China (863 Program) under Contract 2009AA011503, the National Natural Science Foundation of China under Contract 61271135, the National Science and Technology Major Project of the Ministry of Science and Technology of China 2010ZX03007-001-01 and Qualcomm Inc.

The authors are with the State Key Lab of Microwave and Communications, Tsinghua National Laboratory for Information Science and Technology, Tsinghua University, Beijing 100084, China (e-mail: zjzh@tsinghua.edu.cn).

Color versions of one or more of the figures in this communication are available online at http://ieeexplore.ieee.org.

Digital Object Identifier 10.1109/TAP.2013.2287303

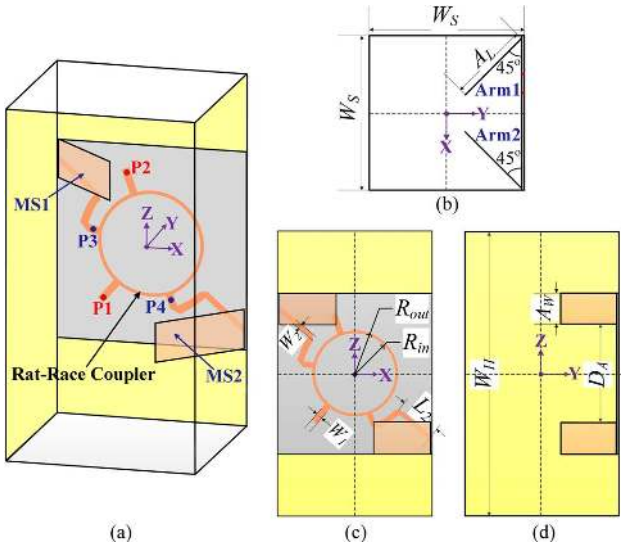

Fig. 1. Antenna geometry: (a) 3D view, and planar views: (b) *xoy* plane, (c) *zox* plane and (d) *zox* plane. Values of the parameters are $\boldsymbol{W_S} = 77.0$, $\boldsymbol{W_H} = 142.0$, $\boldsymbol{A_L} = 40.0$, $\boldsymbol{A_W} = 16.0$, $\boldsymbol{D_A} = 48.0$, $\boldsymbol{R_{in}} = 20.0$, $\boldsymbol{R_{out}} = 21.5$, $W_1 = 3.0$, $W_2 = 2.4$, $\boldsymbol{L_2} = 20.1$ (unit: mm).

II. Antenna Design

A. Antenna Structure

The whole structure of the proposed dual circularly polarized antenna consists of a waveguide with a square aperture, two rectangular metal slices, and a rat-race coupler. Fig. 1 shows the three-dimensional geometry and three planar views, and we can see that the antenna is surrounded by four metallic lateral sides, and the upper $(+\mathrm{Z})$ and lower $(-\mathrm{Z})$ apertures are left open for bidirectional radiations. The width of the square aperture is W_S and the height of the waveguide is W_H. For easy installation of the feeding structure, a 1-mm-thick dielectric substrate ($\varepsilon_r = 2.65$, $\tan\delta = 0.005$) is assembled inside the waveguide. Two identical rectangular metal slices $MS1$ and $MS2$ of length A_L and width A_W are soldered on the front side of the substrate with an intersection angle of 45°. Fig. 1(b) shows that these two metal slices are orthogonal to each other seen from the top plane, and Fig. 1(d) indicates that they are vertically separated by a distance of D_A, which is about a quarter guided wavelength at the desired working frequency. A four-port rat-race coupler is constructed on the substrate with P1 and P2 as inputs and P3 and P4 as outputs to excite the two metal slices, as denoted in Fig. 1(a). The width W_1 of the microstrip line at the four ports of the rat-race coupler is designed to have a characteristic impedance of $Z_0\ \Omega$. The width $(R_{out} - R_{in})$ of the ring-shaped microstrip line is calculated to have an impedance of $(Z_0 \times \sqrt{2})\ \Omega$ and its perimeter is one wavelength and a half, in order to obtain good isolation between the two input ports P1 and P2. The two output ports P3 and P4 are connected to the diagonal line of the two rectangular metal slices. Furthermore, a quarter wavelength impedance transformer with length L_2 and width W_2 at the outputs P3 and P4 is designed for antenna matching, as shown in Fig. 1(c). When the antenna is fed by the input port P1, the two slices can be excited with the same amplitude and phase. However, they are excited with the same amplitude but anti-phase when the input port P2 is selected.

B. Principle of Operation

Taking the structural configuration shown in Fig. 1(a) as an example, the operating principle of the proposed antenna can be explained as follows. When input port P1 is chosen to feed the antenna, the currents on the two slices are excited with the same amplitude and phase, as plotted in Fig. 2(a). The phase of $MS2$ will lag behind that of $MS1$ by 90° when the antenna radiates upwards, and the phase of $MS1$ will lag behind that of $MS2$ by 90° for downward radiation. Therefore, bidirectional LHCP is realized in this antenna configuration by selecting input port P1. Similarly, when the antenna is fed at input port P2, the currents on the two metal slices are excited with the same amplitude, but with a 180° phase difference, which is shown in Fig. 2(b). As a result, bidirectional RHCP can be produced automatically this time. The radiation pattern for both bidirectional LHCP and RHCP is shown in Figs. 3 and 4, respectively. Both senses of CP are available by feeding the antenna at the two different input ports. For either sense of the generated CP, the proposed antenna can naturally radiate CP of the same sense in two different directions. The reason is that a fixed 90° phase shift introduced by the quarter-wavelength separation between the two slices always exists at the two opposite radiating apertures, no matter the two slices are fed in phase or out of phase.

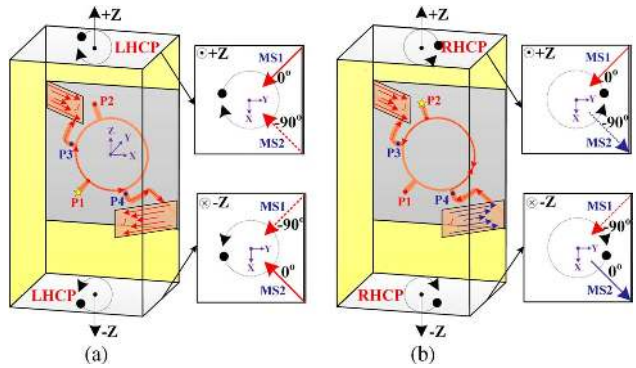

Fig. 2. The generation of both senses of CP by antenna configuration shown in Fig. 1: (a) bidirectional LHCP fed by input port P1, and (b) bidirectional RHCP fed by input port P2.

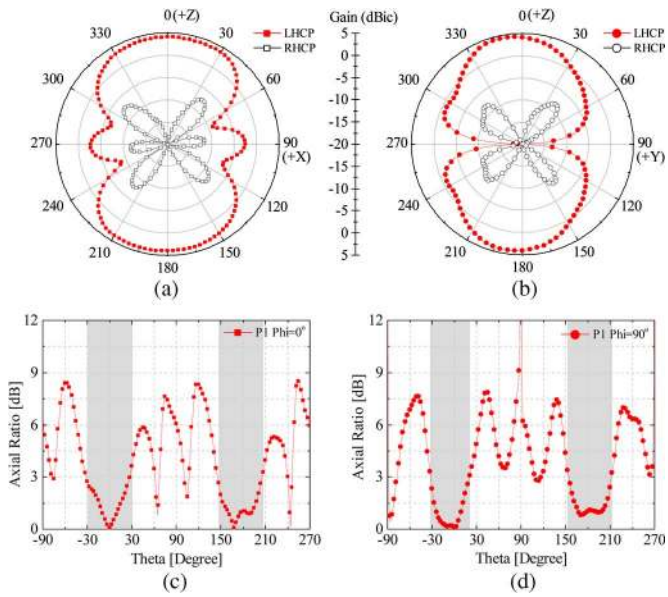

Fig. 3. Bidirectional LHCP radiation characteristic of the proposed antenna at 2.44 GHz when fed by input P1: gain patterns at (a) ***zox*** plane, (b) ***zoy*** plane; and axial ratio beams at (c) ***zox*** plane, (d) ***zoy*** plane.

C. Design Procedure

The procedure to design the proposed antenna is summarized for generality. First, we decide the aperture size W_S of the waveguide

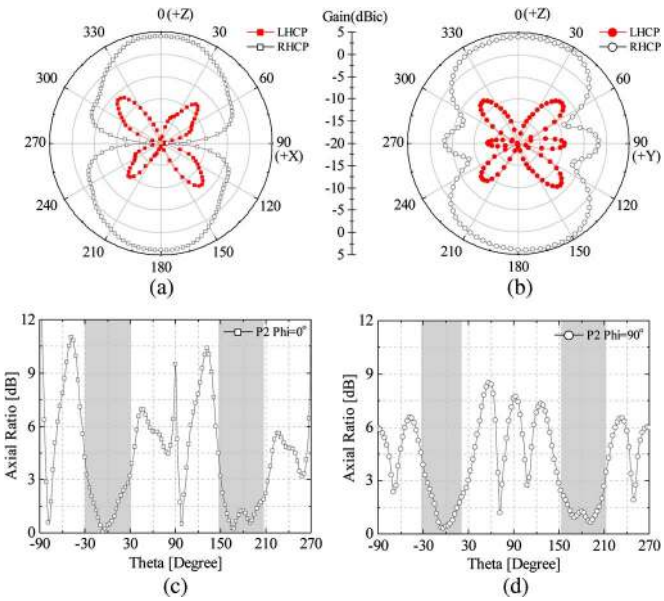

Fig. 4. Bidirectional RHCP radiation characteristic of the proposed antenna at 2.44 GHz when fed by input P2: gain patterns at (a) ***zox*** plane, (b) ***zoy*** plane; and axial ratio beams at (c) ***zox*** plane, (d) ***zoy*** plane.

whose cut-off frequency should be lower than that of the desired operating frequency f_0. The vertical separation D_A of the two rectangular metal slices is then calculated to be a quarter guided wavelength ($\boldsymbol{\lambda_g}/4$). Next, we adjust the waveguide height W_H together with the position of the inserted metal slices to realize bidirectional radiation patterns with identical gain in the two opposite directions. The width A_W and length A_L of the two metal slices are then tuned to obtain a flat frequency characteristic of input impedance at the desired operating band. Finally, we employ a rat-race coupler to feed the two rectangular metal slices with equal amplitude but with 0° or 180° phase difference for both senses of Bi-CP. In addition, a stepped microstrip line with width W_2 and length L_2 is added to make the antenna match for $|\mathrm{S}_{11}| \leq -10$ dB over the whole working band.

To further understand the design process of the proposed antenna, we then investigated the influence of some important parameters on the antenna's performance. For the proposed structure with a computed aperture size W_S, axial ratio of the realized Bi-CP is mainly influenced by the separation D_A between the two metal slices and the height W_H of the waveguide. The quarter-wavelength separation D_A determines the spatial 90° phase difference at the center operating frequency and a larger separation D_A will produce Bi-CP with a minimum axial ratio at a lower frequency, as indicated in Fig. 5(a). The pure 90° phase delay between the two metal slices has little effect on the bandwidth but influences the circularity at a fixed frequency, and shifts the working band. When the position of the two inserted metal slices relative to the middle of the waveguide is kept unchanged for pure 90° phase shift, the waveguide height W_H then has a big influence on the realized axial ratio as well as the bandwidth, as shown in Fig. 5(b). A higher or lower antenna height will not produce good axial ratio, and only a suitable antenna height can realize equal power division at the two different radiating apertures, and thus generate Bi-CP with good purity and bandwidth.

The parameters that significantly influence the antenna's impedance matching include the length A_L and width A_W of the two rectangular metal slices and the widths of the microstrip line in the feeding structure. Fig. 6 shows that dimensions of the two identical slices have a great impact on antenna matching. A longer length A_L will have a

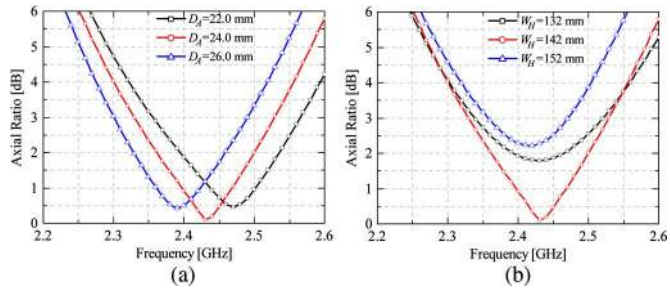

Fig. 5. Axial ratio of the proposed antenna with different dimensions of (a) separation D_A between the two slices; and (b) height of the waveguide W_H.

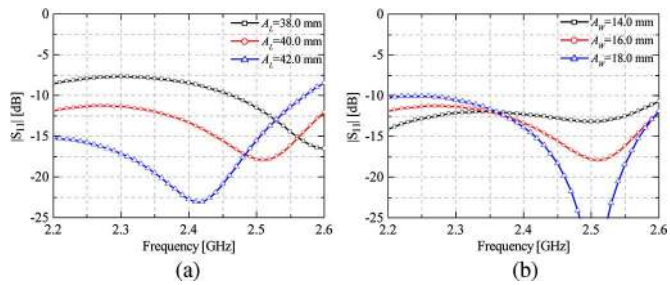

Fig. 6. Reflection coefficient of the proposed antenna with different sizes of the two identical metal slices (a) length A_L; and (b) width A_W.

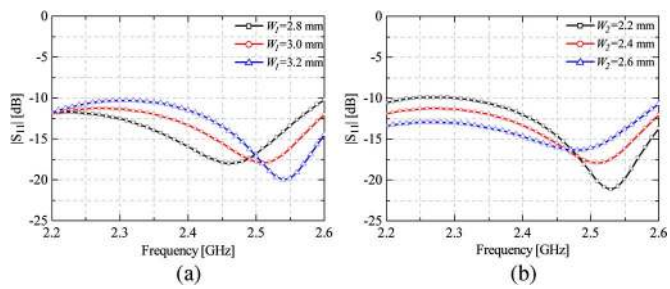

Fig. 7. Reflection coefficient of the proposed antenna with different widths of the feeding microstrip line (a) width W_1 of the rat-race coupler at the input port; and (b) width W_2 of the quarter-wavelength impedance transformer.

better and wider bandwidth at a lower frequency. Meanwhile, an appropriate width A_W can also achieve a good impedance matching for the desired bandwidth. The mutual coupling between the two slices is weak as they are orthogonal to each other, which will cause little influence on the antenna matching. The influence of microstrip width W_1 at the feeding input of the rat-race coupler and W_2 of the quarter-wavelength impedance transformer is plotted in Fig. 7, and we can see that these two parameters have an opposite influence on antenna matching. A wider W_1 will have a better matching at a higher frequency but a wider W_2 makes the matching better at a lower frequency.

III. Results and Discussion

A prototype operating at 2.4-GHz WLAN communication is designed, fabricated, and measured to verify our proposed concept, and the computed values of design parameters are listed in the caption of Fig. 1. The simulation and analysis are realized by Ansoft HFSS based on the finite element method. Figs. 3 and 4 show the simulated bidirectional gain patterns and axial ratio beams when the antenna is fed at input P1 and P2, respectively. When P1 is selected as input port, bidirectional LHCP is generated and 3-dB axial ratio beamwidths of 58° centered at 0° (+Z) and 180° (−Z) directions are both realized in ***zox***

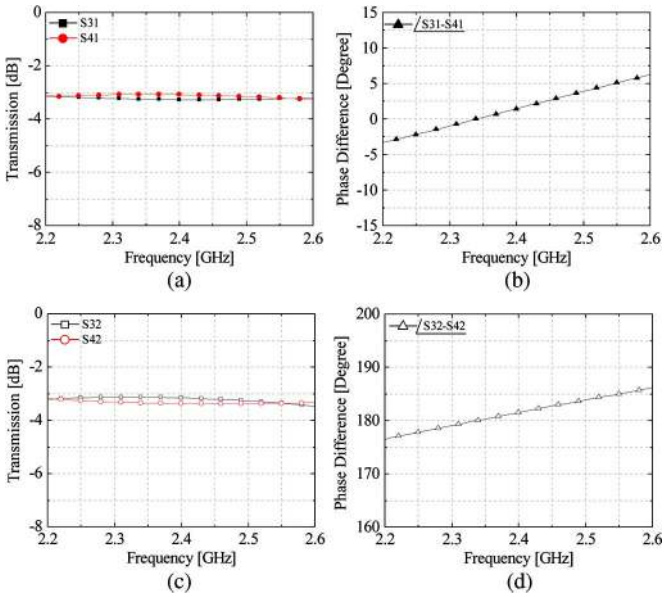

Fig. 8. The output characteristic of the rat-race coupler: (a) amplitude and (b) phase difference of the outputs P3 and P4 when P1 is excited; (c) amplitude and (d) phase difference of the outputs P3 and P4 when P2 is selected.

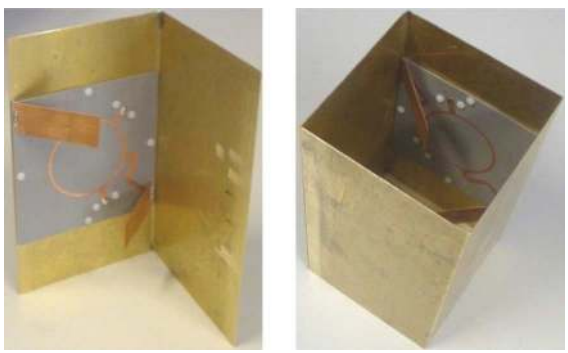

Fig. 9. Photograph of the fabricated prototype: (a) installation of the rat-race coupler and the two rectangular metal slices; (b) the composite antenna.

and ***zoy*** planes. The cross polarization at the center frequency plotted in Figs. 3 and 4 is more than 25 dB lower than the main polarization in the two opposite radiating directions, which means that the degradation of cross polarization by the reflected wave at the waveguide aperture is negligible in our design. The gain variation is smaller than 3 dB within this angular range of the 3-dB axial ratio beamwidth. Meanwhile, an identical maximum gain of about 4.1 dBi is achieved in the two opposite radiating directions. When P2 is selected as input port, bidirectional RHCP is obtained and the radiation characteristic is almost the same as that of LHCP except that the sense of CP is reversed. The main polarization level at the directions of 90° and 270° is a bit high in Fig. 3(a) and Fig. 4(b), which results from the radiation of same-sense CP excited by the currents at the outer surface of the waveguide.

The simulated output characteristic of the designed rat-race coupler is shown in Fig. 8. Within the desired operating band, the output amplitude of P3 and P4 shows a rather small fluctuation with either input excited. When the coupler is excited at the two input ports P1 and P2, the phase difference between the two output ports are 0° and 180° respectively, with a variation of about 5°.

The hand-made prototype is shown in Fig. 9, and we can see that it was assembled simply by soldering two 90°-folded metal plates together. The dielectric substrate with feeding structure and two

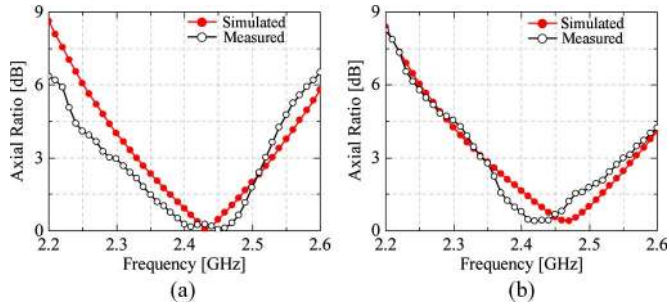

Fig. 10. The simulated and measured axial ratio of the proposed antenna: (a) fed by input port P1; and (b) fed by input port P2.

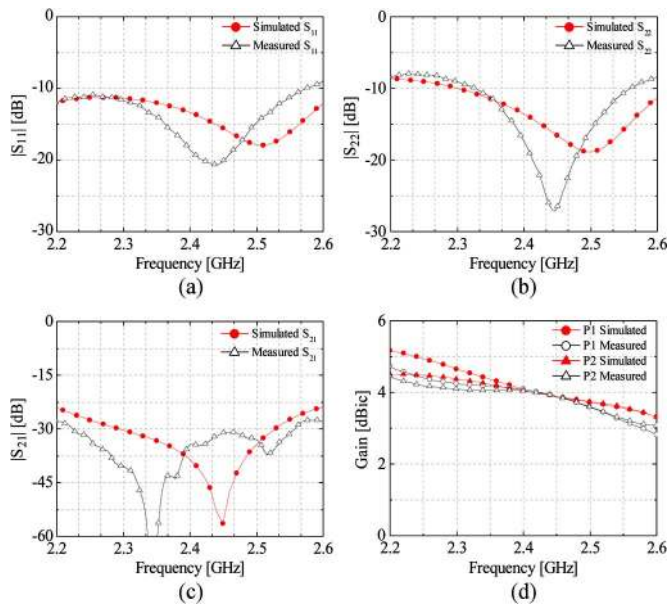

Fig. 11. The simulated and measured reflection coefficient, isolation and gain of the proposed antenna: (a) $|S_{11}|$; (b) $|S_{22}|$; (c) $|S_{21}|$ and (d) gain fed by the two input ports P1 and P2.

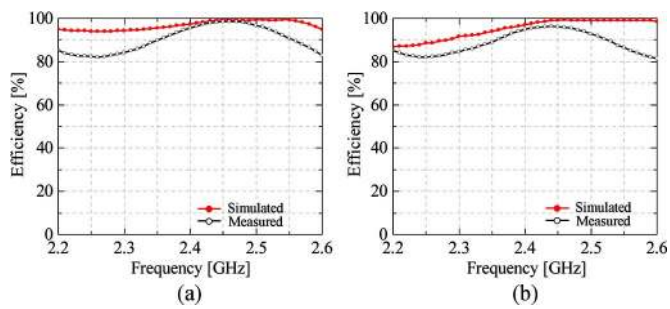

Fig. 12. The simulated and measured efficiency of the proposed antenna: (a) fed by input port P1, and (b) fed by input port P2.

slantly installed metal slices was fixed to one bent plate by nylon screws, as shown in Fig. 9(a). Two 50 Ω SMA connectors installed at the back of the waveguide were used to excite the two inputs of the proposed antenna, with the inner conductor connected to the input microstrip line of the rat-race coupler and the outer shield fastened to the waveguide lateral side. Figs. 10 and 11 compare the measured and the simulated axial ratio, reflection coefficient, isolation and gain of the two input ports, respectively. When the antenna is fed at input P1, the simulated and measured 3-dB axial ratio bandwidth are 200 MHz (8.2%, 2.33–2.53 GHz) and 230 MHz

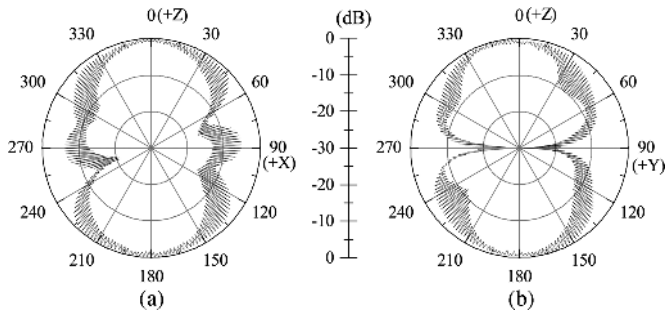

Fig. 13. The measured normalized radiation pattern of LHCP at 2.44 GHz when fed by the input port P1: (a) ***zox*** plane; (b) ***zoy*** plane.

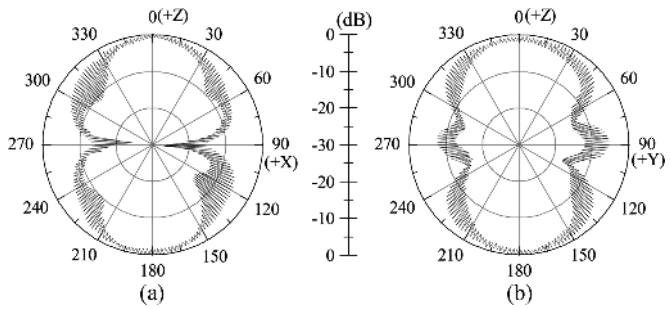

Fig. 14. The measured normalized radiation pattern of RHCP at 2.44 GHz when fed by the input port P2: (a) ***zox*** plane; (b) ***zoy*** plane.

(9.6%, 2.29–2.52 GHz), respectively. The simulated and measured impedance bandwidth for $|S_{11}| \leq -10$ dB are 790 MHz (35.3%, 1.84–2.63 GHz) and 630 MHz (27.8%, 1.95–2.58 GHz), respectively. When the antenna is fed at input P2, the simulated and measured 3-dB axial ratio bandwidth are 220 MHz (9.0%, 2.34–2.56 GHz) and 210 MHz (8.6%, 2.35–2.56 GHz), respectively. The simulated and measured impedance bandwidth for $|S_{22}| \leq -10$ dB are 310 MHz (12.6%, 2.30 GHz to 2.61 GHz) and 240 MHz (9.8%, 2.32–2.56 GHz), respectively. The measured common bandwidth for 10-dB return loss and 3-dB axial ratio at the two feed ports is 230 MHz (9.6%, 2.29–2.52 GHz) and 210 MHz (8.6%, 2.35–2.56 GHz), respectively. Compared to the realization in [13] with a 3-dB axial ratio bandwidth of about 2%, a great enhancement on antenna bandwidth has been achieved by our proposal. Fig. 11(c) shows that the measured isolation between the two feed ports is better than 30 dB over the whole operating band. The measured gain is 3.9 dBic at 2.44 GHz, and a variation of about 1.0 dB is observed within the operating bandwidth, as shown in Fig. 11(d). The decreased gain at the higher frequencies is mainly caused by the raised level of cross polarization. But a more uniform distribution of electric field at the radiating aperture is obtained at the lower frequencies, which could contribute to the relatively higher gain than that at the higher frequencies. The measured in-band efficiency changes in the range of 84–98% and 85–96% for the two inputs, respectively, as shown in Fig. 12. The antenna efficiency within the working band is relatively high because of its low-loss metal structure.

Figs. 13 and 14 show the measured normalized patterns of CP at the two feed ports with a spinning Tx horn. The zigzag in the measured patterns represents the maximum and minimum values of the corresponding axial ratio at a specific angle, and the difference between the two values reflects how big or small the axial ratio is. The outer profile of measured pattern of CP could reflect the spatial distribution of antenna power radiation. The radiation patterns in the whole operating band remain stable. Overall, the measured and the simulated results show good agreement, and the discrepancies can be attributed to the fabricating deviation, the measurement system set up, etc.

IV. Conclusion

A dual-port waveguide antenna with both senses of CP is proposed in this communication. For either sense of CP, the antenna can naturally generate CP of the same sense in two opposite radiating directions. This is realized by two rectangular metal slices that were horizontally perpendicular to each other and vertically separated by a quarter guided wavelength, which introduced a spatial 90° phase shift in two opposite directions. A rat-race coupler was employed to feed the two orthogonal metal slices in phase or out of phase for the realization of dual senses of CP. The proposed antenna alone can function as Tx and Rx antennas simultaneously, which would save much space for the whole system and thus reduce the system complexity. The volume of the proposed antenna can be made smaller by loading the waveguide with dielectric material, and the packaging involves simple mechanical processing like bending, screwing and soldering. A prototype for 2.4-GHz WLAN communications is fabricated and experimentally tested to verify our design. The measured and the simulated results agree well with each other.

References

[1] P. C. Sharma and K. C. Gupta, "Analysis and optimized design of single feed circularly polarized microstrip antennas," *IEEE Trans. Antennas Propag.*, vol. 31, no. 6, pp. 949–955, 1983.

[2] A. Adrian and D. H. Schaubert, "Dual aperture-coupled microstrip antenna for dual or circular polarization," *Electron. Lett.*, vol. 23, no. 23, pp. 1226–1228, 1987.

[3] J. Huang, "A technique for an array to generate circular polarization with linearly polarized elements," *IEEE Trans. Antennas Propag.*, vol. 34, no. 9, pp. 1113–1124, 1986.

[4] E. Aloni and R. Kastner, "Analysis of a dual circularly polarized microstrip antenna fed by crossed slots," *IEEE Trans. Antennas Propag.*, vol. 42, no. 8, pp. 1053–1058, 1994.

[5] W. Dakui, F. Yong, Z. Minghua, and H. Zongrui, "A new kind of millimeter wave dual-circular polarized array," in *Proc. IEEE Int. Symp. on Antennas Propag. & EM Theory (ISAPE)*, 2008, pp. 338–340.

[6] A. Banerjee, V. V. Srinivasan, V. K. Lakshmeesha, and S. Pal, "Novel dual circularly polarized radiating element for spherical phased-array application," *IEEE Antennas Wireless Propag. Lett.*, vol. 8, pp. 826–829, 2009.

[7] M. J. Franco, "A high-performance dual-mode feed horn for parabolic reflectors with a stepped-septum polarizer in a circular waveguide," *IEEE Antennas Propag. Mag.*, vol. 53, pp. 142–146, 2011.

[8] J. A. Ruiz-Cruz, M. M. Fahmi, S. Fouladi, and R. Mansour, "Waveguide antenna feeders with integrated reconfigurable dual circular polarization," *IEEE Trans. Microw. Theory Tech.*, vol. 59, pp. 3365–3374, 2011.

[9] Y.-F. Lin, H.-M. Chen, F.-H. Chu, and S.-C. Pan, "Bidirectional radiated circularly polarized square-ring antenna for portable RFID reader," *Electron. Lett.*, vol. 44, no. 24, pp. 1383–1384, 2008.

[10] S.-P. Pan, J.-Y. Sze, and P.-J. Tu, "Circularly polarized square slot antenna with a largely enhanced axial-ratio bandwidth," *IEEE Antennas Wireless Propag. Lett.*, vol. 11, pp. 969–972, 2012.

[11] J.-Y. Jan, C.-Y. Pan, K.-Y. Chiu, and H.-M. Chen, "Broadband CPW-fed circularly-polarized slot antenna with an open slot," *IEEE Trans. Antennas Propag.*, vol. 61, no. 3, pp. 1418–1422, 2013.

[12] H. lwasaki, "Slot-coupled back-to-back microstrip antenna with an omni- or a bi-directional radiation pattern," *IEE Proc. Microw. Antennas Propag.*, vol. 146, no. 3, pp. 219–223, 1999.

[13] Q.-Y. Zhang, G.-M. Wang, and D.-Y. Xia, "Bidirectional circularly polarized microstrip antenna fed by coplanar waveguide," in *Proc. IEEE Int. Symp. on Antennas Propag. & EM Theory (ISAPE)*, 2006, pp. 1–3.

[14] A. Z. Narbudowicz, X. L. Bao, and M. J. Ammann, "Bidirectional circularly polarized microstrip antenna for GPS applications," in *Proc. Loughborough Antennas and Propagation (LAPC)*, 2010, pp. 205–208.

[15] Y. Zhao, K. Wei, Z. Zhang, and Z. Feng, "A waveguide antenna with bidirectional circular polarizations of the same sense," *IEEE Antennas Wireless Propag. Lett.*, vol. 12, pp. 559–562, 2013.